Rotational-invariant Sturmian-Faddeev *Ansatz* for the solution of H_2^+: A general approach to molecular three-body problems

A. C. Fonseca*
Los Alamos National Laboratory, Los Alamos, New Mexico 87545
and University of Surrey, Guildford, Surrey GU2 5XH, United Kingdom

M. T. Peña
Centro de Física Nuclear, Avenida do Professor Gama Pinto 2, 1699 Lisboa Codex, Portugal
(Received 13 June 1988)

Using a rotational-invariant Faddeev *Ansatz* for the electronic two-center wave function that is written as a sum of terms involving hydrogenic Sturmians and appropriate spherical harmonics coupled to total angular momentum J and parity P, we are able to diagonalize the two-center Hamiltonian to obtain the $1s\sigma_g$, $2s\sigma_g$, $2p\sigma_u$, $2p\pi_u$, and $3d\sigma_g$ electronic energy curves. For 36 Sturmians in the wave function we get energy states that are accurate to six to nine digits for $0<R<20a_0$. All adiabatic corrections are calculated for the $1s\sigma_g$ state and the results compared with previous work by W. Kolos [Acta Phys. Acad. Sci. Hung. **27**, 241 (1969)] and C. L. Beckel, B. D. Hausen, and J. M. Peek [J. Chem. Phys. **53**, 3681 (1970)]. Using the ideas of R. T. Pack and J. O. Hirschfelder [J. Chem. Phys. **49**, 4009 (1968); **52**, 521 (1970); **52**, 4198 (1970)] we calculate the avoided crossing energy gap $\Delta\varepsilon$ between $2s\sigma_g$ and $3d\sigma_g$ curves. For a 36-term Sturmian basis set we get $\Delta\varepsilon=3.27\ \mathrm{cm}^{-1}$ at $R=4.053\,52a_0$. Our work allows for a general approach to the solution of any molecular three-body problem that is applicable independently of the light-particle–heavy-particle interaction and the masses of the two heavier particles.

I. INTRODUCTION

Although there are few molecularlike three-body systems outside molecular physics, the molecular expansion method is a suitable basis to obtain a simple solution to a given nuclear or hadronic three-body problem where two of the particles are heavier than the third one. Because of its nature the molecular approach provides great physical insight and transparency, while at the same time including to some extent three-body degrees of freedom that are needed to achieve a reasonable accuracy in the calculation. This has been shown in a few model calculations with short-range light-particle–heavy-particle interactions[1–3] and in studies of ^{9}Be as a nuclear three-body molecule made up of two α particles and a neutron.[4] Likewise the method has been used to further understand the three-body Efimov effect[5] in a system made up of two heavy particles and a light one. So far, applications to more complex three-body (or three-body-like) systems, and possible generalization to four and more particles, have been limited for lack of a general theoretical framework that easily handles non-Coulomb light-particle–heavy-particle interactions while providing a rotational-invariant solution of the two-center problem that does not rely on the solution of the light-particle Schrödinger equation in the frame where the two heavy particles are fixed in space. It is well known[6] that for Coulomb three-body systems such as H_2^+ or $pp\mu$ the fixed-frame (FF) light-particle wave function separates in elliptic coordinates. Therefore solutions may be obtained with great accuracy either by solving two ordinary differential equations or variationally by using basis functions that take advantage of the above-mentioned separability. For non-Coulomb interactions no such separability can be found and consequently there is no great advantage in using a FF basis set.

In a recent work,[7] hereafter noted as I, we have developed a set of coupled equations for a molecular three-body system involving two identical heavy particles (protons) and a lighter one (electron). Although, for simplicity, we have written the equations for identical heavy particles and attempted to study the H_2^+ molecular ion to test the theory on a well-known problem, the method is sufficiently general to deal with any kind of local or nonlocal light-heavy interaction as well as nonidentical heavy particles. In the work proposed in I the total space-frame (SF) three-body wave function is based on a Faddeev *Ansatz* for the electronic wave function which is obtained from the solution of the Faddeev equations for the electrons moving in the Coulomb field of the two protons that, although kept at distance R, are allowed to rotate with angular momentum L. For the purpose of solving these adiabatic Faddeev equations [Eq. (31) in I] the *e-p* Coulomb t matrix is expressed in a separable form using Sturmians, or Weinberg states.[8] The resulting electronic two-center wave function carries well-defined total angular momentum J and parity P and is expressed as a sum of hydrogenic Sturmians centered on each proton

$$\psi_i^{JP}=\frac{1}{\sqrt{2}}[\bar{\psi}_i^{JP}(\boldsymbol{\rho}_1,\mathbf{R}_1)+\Omega\bar{\psi}_i^{JP}(\boldsymbol{\rho}_2,\mathbf{R}_2)]\ , \tag{1}$$

where, as shown in Fig. 1, $\mathbf{R}_1=-\mathbf{R}_2=\mathbf{R}$, $\boldsymbol{\rho}_1=\boldsymbol{\rho}$ and $\boldsymbol{\rho}_2=\boldsymbol{\rho}+\mathbf{R}$, and Ω is the permutation symmetry of the wave function with respect to the exchange of the two protons. As usual $\Omega=+1$ for even permutation symmetry and $\Omega=-1$ for odd permutation symmetry. The index i denotes the electronic wave function corresponding to a specific molecular energy solution $\bar{\varepsilon}_i^{JP}(R)$ which is the exact solution[7] of the two-center Hamiltonian with the e-p Coulomb potential represented in a separable form through Sturmians. The wave-function Faddeev component reads

$$\bar{\psi}_i^{JP}(\boldsymbol{\rho}_k,\mathbf{R}_k)=\sum_{u=1}^{N_l}\sum_{l,L}\Theta_u^l(\bar{\varepsilon}_i^{JP}(R);|\boldsymbol{\rho}_k|)\mathcal{Y}_{lL}^{JM_J}(\hat{\boldsymbol{\rho}}_k,\hat{\mathbf{R}}_k)\times\bar{G}_i^{JP}(R;ulL)\ , \tag{2}$$

where N_l is the total number of Sturmians used for each e-p relative orbital angular momentum l, and

$$\mathcal{Y}_{lL}^{JM_J}(\hat{\boldsymbol{\rho}}_k;\hat{\mathbf{R}}_k)=\sum_{m,M}Y_{lm}(\hat{\boldsymbol{\rho}}_k)Y_{lm}(\hat{\mathbf{R}}_k)C_{mMM_J}^{lLJ}\ . \tag{3}$$

The sum in l and L runs over all possible values that couple up to J and P and the Θ_u^l are configuration-space hydrogenic Sturmians at energy $\bar{\varepsilon}_i^{JP}(R)$ with angular momentum l and $u-1$ nodes, corresponding to principal quantum number $n=l+u$ (see I for further details). Both $\bar{\varepsilon}_i^{JP}(R)$ and $\bar{G}_i^{JP}(R;ulL)$ emerge from the solution of Eqs. (31a) and (31b) in I. These are homogeneous algebraic equations for the $\bar{G}$ coefficients that for given J, P, and R have a solution at discrete values of $\bar{\varepsilon}$. Since at this stage we are only dealing with the electronic Hamiltonian, $\bar{\varepsilon}_i^{JP}(R)$ is independent of J. For $P\Omega=+1$, $i=1$ denotes the $1s\sigma_g$ molecular energy curve, while $i=2$ and 3 denote the $2s\sigma_g$ and $3d\sigma_g$ curves, respectively. For $P\Omega=-1$, $i=1$ denotes $2p\sigma_u$, while $i=2$ denotes $2p\pi_u$. Although $\bar{\varepsilon}_i^{JP}(R)$ is independent of J, our SF electronic wave function ψ_i^{JP} depends on J through the $\bar{G}_i^{JP}(R;ulL)$ spectator coefficients and the number of independent (lL) pairs one can form for a given J.

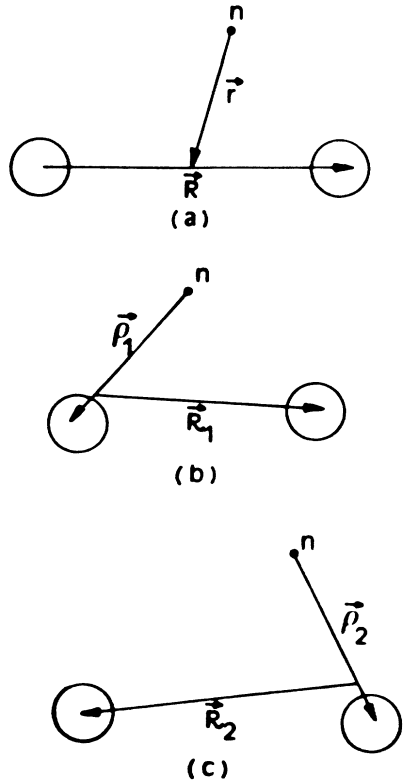

FIG. 1. Jacobi coordinates of the three-body problem.

Using ψ_i^{JP} we calculated next the corresponding Born-Oppenheimer (BO) energy $\varepsilon_i^{JP}(R)$,

$$\varepsilon_i^{JP}(R)=\langle\psi_i^{JP}|h|\psi_i^{JP}\rangle\ , \tag{4}$$

where h is the electronic two-center Hamiltonian

$$h=-\frac{\hbar^2}{2\nu}\nabla_\rho^2-\frac{Ze^2}{\rho}-\frac{Ze^2}{|\boldsymbol{\rho}+\mathbf{R}|}\ , \tag{5}$$

$Z=1$ for H_2^+, $\nu=\mathcal{M}m/(\mathcal{M}+m)$, and $\mathcal{M}(m)$ is the proton (electron) mass. Comparing $\bar{\varepsilon}_i^{JP}(R)$ and $\varepsilon_i^{JP}(R)$ with the best available results for different BO (Refs. 9 and 10) molecular energy curves, we found that both $\bar{\varepsilon}$ and ε are exact at $R=0$ and ∞ and seem to converge to the exact result for $0<R<\infty$, such that at all R $\bar{\varepsilon}>\varepsilon>\varepsilon_{\text{exact}}$. Nevertheless, we also found that the accuracy of the calculation is far from being acceptable by quantum-chemistry standards where energy eigenvalues for H_2^+ are known up to nine significant digits;[11] further difficulties arise from the slow rate with which $\varepsilon_i^{JP}(R)$ approaches the exact solution as the number of hydrogenic Sturmians increases. Denoting $n_{\max}$ the largest hydrogenic principal quantum number $(n=u+l)$ used in the Sturmian expansion, and $l_{\max}$ the largest angular momentum we have included, we found that for $(n_{\max},l_{\max})=(8,7)$,[12] which amounts to a 36-term basis set, the $1s\sigma_g$ energy at $R=2a_0$ ($a_0=0.529\,177\,06$ Å) is only accurate to four digits; at $R=10a_0$ the accuracy of the calculation is reduced to two digits alone, down from three digits when a single-term expansion is used for the Coulomb t matrix. Similar convergence problems appear at large R for $2p\sigma_u$, $2p\pi_u$, $2s\sigma_g$, and $3d\sigma_g$ molecular energy curves. Since we know that for $R>10a_0$ the one-term linear combination of atomic orbitals (LCAO) wave function gives rise to $1s\sigma_g$ electronic energies that are accurate to at least three digits, the above findings clearly suggest that something is wrong with either the Sturmian-Faddeev *Ansatz* for the electronic wave function ψ_i^{JP} or with the way $\bar{\varepsilon}_i^{JP}(R)$ and $\bar{G}_i^{JP}(R;ulL)$ are calculated, that is, through the solution of the adiabatic Faddeev equations [Eq. (31) in I] that result from using a truncated separable representation of the e-p Coulomb t matrix.

In spite of the difficulties encountered in obtaining accurate solutions for the H_2^+ electronic energies, which are possibly due to the long-range nature of the Coulomb potential and the convergence of the Sturmian expansion, three interesting features emerged: (a) the $2s\sigma_g$ and $3d\sigma_g$ curves we obtain seem to be cross inhibited;[7,12] (b) the $2p\pi_u$ and $3d\sigma_g$ potential-energy curves that are responsible for the chemical binding have their minima

correctly reproduced within two-digit accuracy at approximately $R=8a_0$ and $8.8a_0$, respectively,[12] in spite of the large-R distance separation; (c) the method is sufficiently general to handle any kind of local or nonlocal light-heavy interaction which makes any three-body molecularlike system amenable to molecularlike treatment.

The noncrossing feature is particularly puzzling because the Hamiltonian we have in effect diagonalized does not contain the angular momentum operator L^2 in the variable $\hat{\mathbf{R}}$ which in the best adiabatic (BA) method of Pack and Hirschfelder[13] is responsible for the coupling between electronic and nuclear motion that generates cross inhibition. Although in our work we use the electronic Hamiltonian h with a separable representation of the *e-p* potential to generate $\bar{\varepsilon}_i^{JP}$ and $\bar{G}_i^{JP}(R;ulL)$, the SF wave function written in (1), (2), and (3) carries the flexibility needed for the exchange of angular momentum between electronic motion and nuclear motion that cannot be easily expressed in terms of a fixed-frame wave function times a Wigner D function that depends exclusively on $\hat{\mathbf{R}}$ and carriers total angular momentum J such as one usually finds in standard quantum-chemistry books. Furthermore, since the Sturmian expansion is known to converge[14] for short-range potentials, the problems we found at large R should disappear for three-body molecular systems where the light-heavy interaction is short range. Also, improved accuracy and faster rate of convergence as the number of Sturmians increases should be found in those cases.

In order to improve on the previous work and obtain accurate results for long-range light-heavy interactions two directions may be undertaken: (a) solve the adiabatic two-center Faddeev equations using the full *e-p* Coulomb potential; (b) use a SF two-center Sturmian *Ansatz* similar to the one written in (1), (2), and (3) and calculate $\bar{\epsilon}$ and G through direct diagonalization of the Hamiltonian h shown in (4) without setting up a separable representation for the *e-p* potential. Since the first approach would most certainly lead to numerical difficulties we do not feel prepared to handle at this time, we choose the second alternative, which is more in line with the work developed in I and the variational methods used in quantum chemistry. The major difference relative to quantum-chemistry methods lies in the nature of the *Ansatz,* particularly in the way one achieves a SF representation for the electronic wave function carrying good total angular momentum J and parity P. Compared to the work developed in I, by using (1), (2), and (3) to diagonalize h, one gets $\bar{\varepsilon}_i^{JP}(R)=\varepsilon_i^{JP}(R)$ and new $G_i^{JP}(R;ulL)$ coefficients.

Since our electronic wave function satisfies the requirements needed to perform a BA calculation, improvements may be easily included by diagonalizing $h+L^2$ instead of h alone, leading to the calculation of the avoided crossing energy gap between $2s\sigma_g$ and $3d\sigma_g$ curves which have the same symmetry and an improved calculation of the adiabatic corrections.[15,16] In addition, since the method proposed here, as well as in I, is independent of the light-heavy interaction one uses, any three-body molecularlike system becomes easily amenable to rotational-invariant molecularlike treatment, where adiabatic as well as nonadiabatic corrections due to appropriate choice of Jacobi variables and coupling to higher molecular states may be easily accounted for. Recent work in this direction consisted in a very successful application of the work developed in I to the study of ^{9}Be as a three-body nuclear molecule made up of $\alpha+n+\alpha$.[17] Our aim here is to test the method in the presence of long-range Coulomb forces where very accurate results are known. In Sec. II we write the matrix equations we solve to diagonalize h with the present choice for the electronic *Ansatz* and show the corresponding results for $\varepsilon_i^{JP}(R)$ and $G_i^{JP}(R;ulL)$. In Sec. III we calculate all adiabatic corrections due to Coriolis coupling effects in L^2, mass polarization corrections to the electronic kinetic energy, and derivatives of ψ_i^{JP} with respect to R. An improved adiabatic calculation of L^2 and the avoided crossing energy gap between $2s\sigma_g$ and $3d\sigma_g$ curves is also reported in Sec. III. Finally, in Sec. IV we draw some conclusions.

II. DIAGONALIZATION OF THE ELECTRONIC HAMILTONIAN

As mentioned before, we take the Faddeev *Ansatz* for the electronic wave function that is suggested from our previous work in Ref. 7 and that we believe is more flexible than standard quantum-chemistry electronic *Ansätze* in coupling the electronic motion to the nuclear motion. Nevertheless, unlike in I, we use such an *Ansatz* to diagonalize the two-center Hamiltonian expressed in (5), instead of solving the Faddeev equations that result from a separable representation of the *e-p* Coulomb potential. Therefore one starts by writing ψ^{JP} as

$$\psi^{JP}(\boldsymbol{\rho},\mathbf{R})=\sum_c \phi^{JP}(\boldsymbol{\rho},\mathbf{R};c)G^{JP}(R;c)\ , \tag{6}$$

where the summation in c runs over all possible combinations of u, l, and L, and

$$\phi^{JP}(\boldsymbol{\rho},\mathbf{R};c)=\frac{1}{\sqrt{2}}[\Theta_u^l(\varepsilon;\rho_1)Y_{lL}^{JM_J}(\hat{\boldsymbol{\rho}}_1,\hat{\mathbf{R}}_1) +\Omega\Theta_u^l(\varepsilon;\rho_2)y_{lL}^{JM_J}(\hat{\boldsymbol{\rho}}_2,\hat{\mathbf{R}}_2)]\ , \tag{7}$$

$$\mathbf{R}_1=-\mathbf{R}_2=\mathbf{R}\ , \tag{8a}$$

$$\boldsymbol{\rho}_1=\boldsymbol{\rho}\ , \tag{8b}$$

$$\boldsymbol{\rho}_2=\boldsymbol{\rho}+\mathbf{R}\ . \tag{8c}$$

Since most calculations we undertake are more easily done in momentum space, we write the configuration-space hydrogenic Sturmian Θ_u^l as

$$\Theta_u^l(\varepsilon;\rho)=\sqrt{4\pi}\int\frac{q^2dq}{2\pi^2}\left[\varepsilon-\frac{\hbar^2}{2\nu}q^2\right]^{-1}\xi_u^l(\varepsilon;q)j_l(q\rho)\ , \tag{9}$$

where ν is the separated atom reduced mass that is needed to obtain the correct dissociation limit.

The ξ_u^l are given in Appendix C of I, and the j_l are spherical Bessel functions of order l. Next we use ψ^{JP} in

$$h\psi^{JP}=\varepsilon\psi^{JP}\ , \tag{10}$$

substitute (5) and (6) in (10), multiply on the left by $\phi^{JP}(\boldsymbol{\rho},\mathbf{R};c')$, and integrate in $d^3\rho$ and $d\Omega_R$ to obtain a matrix equation

$$\sum_c [B^{c'c}(R;JP)+v^{c'c}(R;JP)]G^{JP}(R;c)=0, \tag{11}$$

where

$$B^{c'c}(R;JP)=\left\langle \phi^{JP}(\boldsymbol{\rho},\mathbf{R};c') \left| \left[-\varepsilon-\frac{\hbar^2}{2\nu}\nabla_\rho^2 \right] \right| \phi^{JP}(\boldsymbol{\rho},\mathbf{R};c) \right\rangle , \tag{12}$$

and

$$v^{c'c}(R;JP)=\left\langle \phi^{JP}(\boldsymbol{\rho},\mathbf{R};c') \left| \left[-\frac{Ze^2}{\rho}-\frac{Ze^2}{|\boldsymbol{\rho}+\mathbf{R}|} \right] \right| \phi^{JP}(\boldsymbol{\rho},\mathbf{R};c) \right\rangle . \tag{13}$$

Equation (11) is a homogeneous algebraic equation whose solution for a given J, P, and R only exists at discrete values of ε denoted henceforward as $\varepsilon_i^{JP}(R)$. The corresponding eigenvalues are $G_i^{JP}(R;c)$, which are spectator coefficients that account for the weight with which each Sturmian enters in the two-center electronic wave function. Since the Sturmian eigenfunctions satisfy very simple properties (see Appendixes A and C in I), most matrix elements are easily evaluated. One gets

$$B^{c'c}(R;JP)=\delta_{u'u}\delta_{l'l}\delta_{L'L}-\Omega B^{JP}(R;c'c)\ , \tag{14}$$

where

$$B^{JP}(R;c'c)=\sum_{\mathcal{L}}\chi_{\mathcal{L}}^{JP}(l'L';lL)\times\int\frac{q^2dq}{2\pi^2}\frac{\xi_{u'}^{l'}(\varepsilon;q)\xi_u^l(\varepsilon;q)}{\varepsilon-\frac{\hbar^2}{2\nu}q^2}j_{\mathcal{L}}(qR)\ . \tag{15}$$

The χ is the angular momentum coupling coefficient given by

$$\chi_{\mathcal{L}}^{JP}(l'L';lL)=x(-1)^{J+L'+l}\hat{\mathcal{L}}^2\hat{l}\hat{l}'\hat{L}\hat{L}'\begin{bmatrix} l & \mathcal{L} & l' \\ 0 & 0 & 0 \end{bmatrix}\times\begin{bmatrix} L & \mathcal{L} & L' \\ 0 & 0 & 0 \end{bmatrix}W(l'lL'L;\mathcal{L}J)\ , \tag{16a}$$

where x is an extra phase

$$x=(-1)^{(l+l'+\mathcal{L})/2}\ , \tag{16b}$$

$\left(\begin{smallmatrix} a & b & c \\ 0 & 0 & 0 \end{smallmatrix}\right)$ is a 3-j coefficient, and W is a Racah. As for v one again follows the work in I to obtain

$$v^{c'c}(R;JP)=-\eta_u^l(\varepsilon)\delta_{u'u}\delta_{l'l}\delta_{L'L}+\Omega[\eta_{u'}^{l'}(\varepsilon)+\eta_u^l(\varepsilon)]B^{JP}(R;c'c)+V^{JP}(R;c'c)\ , \tag{17}$$

where η_u^l is the corresponding Sturmian eigenvalue

$$(\eta_u^l)^{-1}=\frac{(u+l)}{Z}\sqrt{-\varepsilon}\ , \tag{18}$$

$$V^{JP}(R;c'c)=\sum_{\mathcal{L}}\bar{\chi}_{\mathcal{L}}^{JP}(l'L';lL)\times\int_0^\infty\rho^2d\rho\,\Theta_{u'}^{l'}(\varepsilon;\rho)v_{\mathcal{L}}(\rho,R)\Theta_u^l(\varepsilon;\rho)\ , \tag{19}$$

and

$$\bar{\chi}_{\mathcal{L}}^{JP}(l'L';lL)=x(-1)^{l+L'}(\hat{\mathcal{L}})^{-2}\chi_{\mathcal{L}}^{JP}(l'L';lL)\ . \tag{20}$$

The χ is given by (16a), x by (16b), the Θ's are taken from (9), and

$$v_{\mathcal{L}}(\rho,R)=-Ze^2\frac{r_<^{\mathcal{L}}}{r_>^{\mathcal{L}+1}}\ , \tag{21}$$

with $r_<=\min\{\rho,R\}$ and $r_>=\max\{\rho,R\}$. Therefore the integral in (19) has always to be broken in two regions $[0,R]$ and $[R,\infty]$.

As mentioned before, Eq. (11) is a secular equation whose solution only exists at a discrete set of $\varepsilon_i^{JP}(R)$. Therefore given J, P, and R one finds the values of ε for which the determinant

$$|B(R;JP)+v(R;JP)|=0\ . \tag{22}$$

As in I the energy eigenvalues $\varepsilon_i^{JP}(R)$ are independent of J as one expects from the diagonalization of the electronic Hamiltonian alone, but the spectator coefficients $G_i^{JP}(R;c)$ are strongly J dependent, because the number of channels c involved in the calculation depends on J. As usual the G's resulting from (11) are known up to an overall normalization constant that is fixed by requiring that

$$\langle\psi_{i'}^{JP}|\psi_i^{JP}\rangle=\delta_{i'i} \tag{23}$$

at all R. For $\Omega P=+1$ the lowest energy solution we find is the $1s\sigma_g$ molecular curve which is denoted as $i=1$. In Table I we show $\varepsilon_1^{J+}(R)$ versus R and compare with the most precise results of Madsen and Peek.[10] Unlike in I,

TABLE I. $\varepsilon_1^{J^P}(R)$ (in Ry) vs R for increasing (n_{max},l_{max}). The exact $1s\sigma_g$ results are shown for comparison.

R/a_0	(1,0)	(2,1)	(3,2)	(5,4)	(8,7)	Exact (Ref. 10)
0	4.000 000 00	4.000 000 00	4.000 000 00	4.000 000 00	4.000 000 00	4.000 000 00
1	2.858 683 84	2.900 642 27	2.903 212 41	2.903 557 26	2.903 571 56	2.903 572 63
2	2.118 367 32	2.203 571 62	2.205 086 02	2.205 257 55	2.205 268 13	2.205 268 43
3	1.735 736 98	1.819 922 62	1.821 567 64	1.821 786 36	1.821 792 26	1.821 792 39
4	1.524 997 22	1.589 494 21	1.591 970 33	1.592 166 14	1.592 169 70	1.592 169 77
5	1.401 997 13	1.446 056 96	1.448 700 89	1.448 838 13	1.448 840 56	1.448 840 59
10	1.192 003 29	1.200 915 85	1.201 141 50	1.201 157 35	1.201 157 45	1.201 157 46
15	1.129 401 91	1.133 401 17	1.133 430 40	1.133 431 21	1.133 431 21	1.133 431 21
20	1.097 722 56	1.100 019 82	1.100 028 40	1.100 028 49	1.100 028 49	1.100 028 52

one finds that the one-term approximation is very poor, but as the number of terms in the Sturmian representation of the wave function increases, $\varepsilon_1^{J+}(R)$ converges quickly and monotonically to the results of Madsen and Peek at all R. For $(n_{max},l_{max})=(5,4)$, which amounts to a 15-term basis set, we get at least five-digit accuracy at all R, which is a great deal more than we ever got in I with a 36-term basis set.[12] For $(n_{max},l_{max})=(8,7)$ one now gets better then seven-digit accuracy at all R. The corresponding potential-energy curve defined as

TABLE II. Weight factors $G_1^{0+}(R;ull)$ at $R=8a_0$ for increasing (n_{max},l_{max}). In the last column we show the corresponding results from Ref. 12 for (7,6).

	This work			From Ref. 12
G's	(3,2)	(5,4)	(7,6)	(7,6)
$1s$	1.477	1.475	1.475	1.28
$2s$	-1.709×10^{-1}	-1.688×10^{-1}	-1.683×10^{-1}	-1.18×10^{-1}
$3s$	1.741×10^{-2}	1.622×10^{-2}	1.612×10^{-2}	4.50×10^{-2}
$4s$		-1.473×10^{-3}	-1.773×10^{-4}	-2.74×10^{-2}
$5s$		-3.277×10^{-5}	1.685×10^{-4}	2.70×10^{-2}
$6s$			-2.224×10^{-5}	-1.76×10^{-2}
$7s$			-7.492×10^{-6}	4.80×10^{-4}
$8s$				
$2p$	5.088×10^{-2}	4.920×10^{-2}	4.884×10^{-2}	4.76×10^{-1}
$3p$	-2.368×10^{-2}	-2.243×10^{-2}	-2.233×10^{-2}	-3.72×10^{-2}
$4p$		3.646×10^{-3}	4.035×10^{-3}	4.08×10^{-2}
$5p$		-9.816×10^{-6}	-3.646×10^{-4}	-4.67×10^{-2}
$6p$			1.014×10^{-5}	3.18×10^{-2}
$7p$			-5.482×10^{-6}	-2.56×10^{-3}
$8p$				
$3d$	1.305×10^{-2}	1.247×10^{-2}	1.235×10^{-2}	2.52×10^{-2}
$4d$		-5.681×10^{-3}	-5.925×10^{-3}	-4.45×10^{-2}
$5d$		4.658×10^{-4}	8.862×10^{-4}	5.77×10^{-2}
$6d$			3.559×10^{-5}	-4.31×10^{-2}
$7d$			1.957×10^{-5}	7.88×10^{-3}
$8d$				
$4f$		4.570×10^{-3}	4.631×10^{-3}	3.17×10^{-2}
$5f$		-1.423×10^{-3}	-1.783×10^{-3}	-5.44×10^{-2}
$6f$			3.421×10^{-5}	5.08×10^{-2}
$7f$			1.920×10^{-5}	-1.73×10^{-2}
$8f$				
$5g$		1.741×10^{-3}	1.935×10^{-3}	3.65×10^{-2}
$6g$			-4.234×10^{-4}	-5.11×10^{-2}
$7g$			-8.344×10^{-5}	2.98×10^{-2}
$8g$				
$6h$			7.840×10^{-4}	3.85×10^{-2}
$7h$			-1.290×10^{-5}	-4.03×10^{-2}
$8h$				
$7i$			2.773×10^{-4}	3.80×10^{-2}
$8i$				
$8j$				

$$E_i^{J^+}(R)=\varepsilon_1^{J^+}(R)+\frac{(Ze)^2}{R}-\varepsilon_1^{J^+}(\infty) \quad (24)$$

shows the well-known minima very near $R=2a_0$. For $R=2a_0$, $E_1^{J^+}(R)=0.102\,634\,06$ a.u., while Madsen and Peek obtain $E_{1s\sigma_g}(R)=0.102\,632\,1$ a.u. Our previous energy result from I at $R=2a_0$ is 0.102 435 a.u., which agrees with the present result only on the first four digits. Two additional significant digits are obtained by the present variational approach based on a similar wave-function *Ansatz*. The normalized spectator coefficients $G_1^{0+}(R;c)$ are shown in Table II at $R=8a_0$ for increasing $(n_{\max},l_{\max})$. For (7,6) we show the corresponding results from I. Not only are the present weights considerably different from the previous ones, but we also find that the convergence pattern is different. Although as discussed in Sec. III, the numerical difficulties one encounters here are considerably bigger than in I, where the solution of the corresponding homogeneous equation is numerically more stable, particularly for large basis sets $(n_{\max},l_{\max})>(5,4)$ and intermediate values of R $(1a_0<R<8a_0)$, the present findings give a clear indication why the previous work lacked the accuracy that is needed to deal with long-range potentials. Since the Coulomb potential is a long-range potential, and the Sturmian separable representation of the Coulomb potential is a sum of short-ranged terms, the method developed in I is not accurate enough to generate through the solution of the Faddeev equations energies and wave functions that are acceptable by quantum-chemistry standards. Even if in I some apparent convergence seems to exist for the energy eigenvalues, the wave function is well away from a converged status. On the contrary, if the same Faddeev-like *Ansatz* is used in the context of a variational calculation to diagonalize the full Hamiltonian, improved results are obtained. Although this may look like a trivial point, as far as we know, it is not mentioned or suggested in the literature where Faddeev calculations involving atomic or molecular systems have been done in the past. The results obtained here excel the precision of any calculation using N-body methods, including the one by Ford and Levin[18] based on the solution of channel-permuting-array (CPA) theory using finite element methods, and seem to indicate that for long-ranged potentials one may get improved accuracy by using a standard Faddeev global *Ansatz* as suggested by a given separable representation of the underlying potential, in a variational-like diagonalization of the original Hamiltonian. Because the above-chosen *Ansatz* still factorizes with respect to the relative *e-p* momentum, the equations that are solved here have the same dimensionality as the Faddeev equation obtained in I but, because we take the full *e-p* Coulomb potential instead of a separable representation of it, extra accuracy is gained. The price one pays is the calculation of one extra integral involving a multipole expansion of the light-heavy particle interaction. Here also lies the advantage of the Sturmian *Ansatz* which makes the calculation of most matrix elements a very easy task. Since we have not used any special numerical technique to handle integrals over products of highly oscillatory form factors and Bessel functions, beyond making sure we had a sufficient number of mesh points to allow for eight or nine stable digits in the energy eigenvalues, we expect to gain further accuracy and speed in the calculation by introducing some numerical refinements. Nevertheless, using a 36-term basis set at each R the calculation of one energy eigenvalue and corresponding wave function as well as all adiabatic corrections described in Sec. III takes about 20 sec on the Cray XMP48.

Next we study the contribution of high l's to the $1s\sigma_g$ energy at different values of R. This is shown in Table III for $(n_{\max},l_{\max})$ ranging from (8,7) to (8,0). As expected for very small $(R<0.5a_0)$ or very large $(R>10a_0)$ values of R the contribution of $l>3$ *e-p* angular momentum contributions only changes the seventh significant digit. In between, one may need to go as high as $l=5$ to obtain eight significant digits, which implies a 33-term basis set.

If one now studies the excited molecular energy states corresponding to $2p\sigma_u$, $2p\pi_u$, $2s\sigma_g$, and $3d\sigma_g$ one also finds considerably improved accuracy over the work performed in I. In Tables IV–VI the results of the present calculation are shown at some values of R and for an increasing number of terms in the Sturmian expansion of the wave function. When compared with the best-known exact results[10] one finds that they converge monotonically at all R and that for the largest $(n_{\max},l_{\max})$ we have calculated one gets five- to nine-digit accuracy depending on which state or R value one considers. As in I, we find that for a given $(n_{\max},l_{\max})$ the $2s\sigma_g$ and $3d\sigma_g$ curves are cross inhibited. Nevertheless, as shown in Fig. 2, the cross inhibition gap $\Delta\varepsilon$ decreases as $(n_{\max},l_{\max})$ increases to become 2.73×10^{-7} a.u. (0.0599 cm^{-1}) at $R=4.0535a_0$ with $(n_{\max},l_{\max})=(8,7)$. Because at (8,7) the size of the gap is within the precision of the calculation we cannot positively ascertin whether the two calculated curves cross or not. Therefore it is possible that in the limit of an infinite number of basis states we may get curve crossing as one expects. The only possible way to sort this out is diagonalizing $h+L^2$ as suggested in Ref. 13 to find out if the resulting cross inhibition gap is bigger than the result quoted above and stable against changes in the number of terms in the basis state. This was done below in Sec. III where for $(n_{\max},l_{\max})=(8,7)$ we find $\Delta\varepsilon=1.49\times10^{-5}$ a.u. (3.27 cm^{-1}) at $R=4.053\,52a_0$. Although further details are given below, this indicates that L^2 is indeed responsible for breaking the symmetry that leads to curve crossing in the BO approximation.[13] Nevertheless, because our original *Ansatz* already breaks that symmetry one needs a large basis set to restore it when one diagonalizes h alone. The difference between both calculations is shown in Fig. 3 for $(n_{\max},l_{\max})=(8,7)$.

Therefore both the work proposed in I and here allow for a very general rotational-invariant treatment of the two-center potential problem which is based on a Sturmian-Faddeev *Ansatz* for the SF light-particle wave function that may be used independently of the chosen light-heavy interaction. For short-range potentials the method proposed in I should converge well as the number of separable terms increases, as one finds in standard three-body calculations.[19] For long-range potentials

TABLE III. $\varepsilon_1^{JP}(R)$ (in Ry) vs l_{max} for $n_{max}=8$ and different values of R.

R/a_0 (n,l)	0.2	2	4	8	15	20
(8,7)	3.857 234 413	2.205 268 130	1.592 169 703	1.255 140 774	1.133 431 211	1.100 028 445
(8,6)	3.856 234 413	2.205 268 130	1.592 169 703	1.255 140 774	1.133 431 211	1.100 028 445
(8,5)	3.857 234 413	2.205 268 130	1.592 169 701	1.255 140 763	1.333 431 211	1.100 028 445
(8,4)	3.857 234 413	2.205 268 125	1.592 169 607	1.255 140 713	1.133 431 211	1.100 028 445
(8,3)	3.856 234 411	2.205 267 856	1.592 167 970	1.255 140 077	1.133 431 211	1.100 028 444
(8,2)	3.857 234 408	2.205 256 385	1.592 137 465	1.255 131 870	1.133 431 133	1.100 028 437
(8,1)	3.856 234 340	2.204 813 775	1.591 389 000	1.255 024 239	1.133 429 339	1.100 028 152
(8,0)	3.856 897 784	2.181 886 479	1.576 249 398	1.253 517 957	1.133 339 830	1.100 000 002

TABLE IV. $\varepsilon_1^{J-}(R)$ (in Ry) vs R for increasing (n_{max},l_{max}). The exact $2p\sigma_u$ results are shown for comparison.

R/a_0	(2,1)	(3,2)	(5,4)	Exact (Ref. 10)
0	1.000 000 00	1.000 000 00	1.000 000 00	1.000 000 00
1	1.129 225 46	1.129 579 43	1.129 623 62	1.129 627 25
2	1.334 756 03	1.335 033 18	1.335 067 19	1.335 068 78
3	1.402 710 44	1.402 824 01	1.402 836 34	1.402 836 66
4	1.391 014 99	1.391 096 02	1.391 101 21	1.391 101 28
5	1.354 477 59	1.354 580 06	1.354 583 23	1.354 583 20
10	1.199 693 23	1.199 800 22	1.199 802 13	1.199 802 13
15	1.133 389 09	1.133 416 95	1.133 417 46	1.133 417 46

TABLE V. $\varepsilon_2^{J-}(R)$ (in Ry) vs R for increasing (n_{max},l_{max}). The exact $2p\pi_u$ results are shown for comparison.

R/a_0	(2,1)	(3,2)	(5,4)	Exact (Ref. 10)
0	1.000 000 00	1.000 000 00	1.000 000 00	1.000 000 00
1	0.946 750 82	0.947 963 56	0.948 192 76	0.948 215 91
2	0.847 952 76	0.856 716 51	0.857 517 77	0.857 543 64
3	0.751 599 51	0.771 971 10	0.772 869 84	0.772 887 70
4	0.670 102 86	0.700 850 45	0.701 629 20	0.701 649 29
5	0.604 492 80	0.641 910 12	0.642 746 44	0.642 769 62
10	0.432 125 15	0.461 907 89	0.465 412 16	0.465 432 58
15	0.370 984 43	0.384 742 91	0.387 074 59	0.387 090 72

TABLE VI. $\varepsilon_2^{J+}(R)$ and $\varepsilon_3^{J+}(R)$ vs R for increasing (n_{max},l_{max}). The exact $2s\sigma_g$ and $3d\sigma_g$ results are shown for comparison.

R/a_0	(5,4)	(8,7)	Exact $2s\sigma_g$ Ref. 10	Exact $3d\sigma_g$ Ref. 10	(8,7)	(5,4)
0	1.000 000 00	1.000 000 00	1.000 000 00	0.444 444 44	0.444 444 44	0.444 444 44
1	0.845 679 89	0.845 840 34	0.845 849 17	0.450 369 38	0.450 369 31	0.450 368 76
2	0.721 667 64	0.721 725 37	0.721 729 75	0.471 555 26	0.471 554 90	0.471 549 32
3	0.637 712 44	0.637 771 31	0.637 774 10	0.515 008 61	0.515 008 33	0.514 999 75
4	0.576 965 01	0.577 028 14	0.577 029 73	0.571 447 58	0.571 447 53	0.571 444 76
5	0.612 025 29	0.612 026 15	0.531 011 63	0.612 026 15	0.531 010 50	0.530 957 09
6	0.624 987 26	0.624 989 64	0.495 109 18	0.624 989 65	0.495 108 30	0.495 066 96
7	0.616 836 71	0.616 841 10	0.466 558 80	0.616 841 13	0.466 558 14	0.466 525 07
8	0.597 017 35	0.597 023 25	0.443 554 67	0.597 023 28	0.443 554 20	0.443 525 95
9	0.572 216 62	0.572 223 57	0.424 824 93	0.572 223 61	0.424 824 62	0.424 799 93
10	0.546 226 95	0.546 234 84	0.409 421 25	0.546 234 88	0.409 421 03	0.409 400 02
15	0.438 281 11	0.438 296 08	0.361 809 87	0.438 296 12	0.361 809 84	0.361 804 77
20	0.375 515 27	0.375 532 14	0.336 998 60	0.375 532 16	0.336 998 60	0.336 997 59

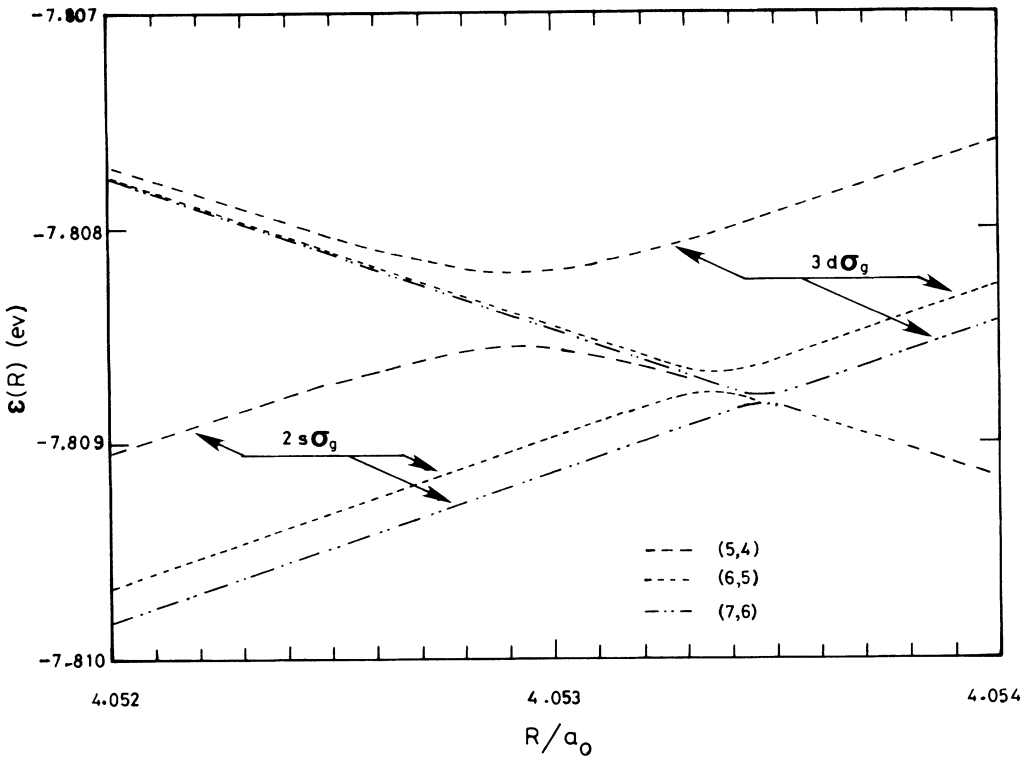

FIG. 2. $\varepsilon_2^{JP}(R)$ and $\varepsilon_3^{JP}(R)$ vs R for increasing $(n_{\max}, l_{\max})$.

and/or considerable accuracy one may still use the same Sturmian-Faddeev *Ansatz* but in the context of a variational calculation. As a consequence of this work any three-body molecularlike system becomes amenable to molecularlike treatment, as long as one can find the Weinberg states or Sturmians of the underlying light-heavy particle interaction. For some potentials such as harmonic oscillator, Hulthen, and Coulomb this is an easy task. For others one may have to solve an eigenvalue problem at each ε (see I and references therein for details).

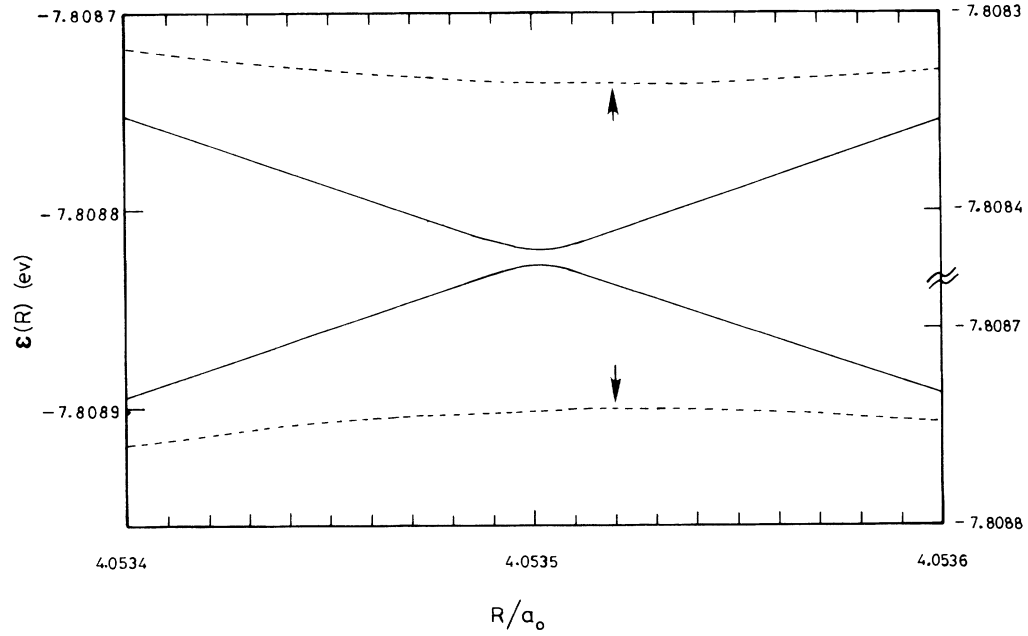

FIG. 3. $\varepsilon_2^{JP}(R)$ and $\varepsilon_3^{JP}(R)$ vs R for $(n_{\max}, l_{\max})=(8,7)$. While the solid line corresponds to diagonalizing h alone, the dashed line corresponds to diagonalizing $h+L^2/2\bar{\mu}R^2$. The arrow indicates the position of the minimum. The left scale corresponds to the solid line, while the scale on the right corresponds to the dashed line.

III. ADIABATIC CORRECTIONS

Using the $1s\sigma_g$ electronic energy curve and wave function developed above we now proceed to calculate the adiabatic corrections that are needed for an accurate calculation of the H_2^+ spectra. In the present work we use the standard form of the BA *Ansatz* for the three-body wave function

$$\Psi^{JP}(\boldsymbol{\rho},\mathbf{R})=\psi^{JP}(\boldsymbol{\rho},\mathbf{R})\Phi^{JP}(R) \tag{25}$$

instead of the one proposed in Eq. (41) of I which leads to a set of coupled differential equations in the variable R. Two reasons lead us to this choice at this time: (a) we want to be able to compare some of the adiabatic corrections predicted in the framework of this *Ansatz* with the well-known corrections calculated years ago by Kalos[20] and Beckel *et al.*;[21] (b) being in the process of developing a computer code for the solution of coupled differential equations at negative energies using the spline expansion method that reduces the task to the solution of a generalized eigenvalue problem, we want to make sure that our method leads to reasonable results for the cases for which one already knows the answer. Therefore using (25) in

$$H\Psi=E\Psi\ , \tag{26}$$

where H is the full three-body Hamiltonian

$$H=-\frac{\hbar^2}{2\bar{\mu}}\nabla_R^2+\frac{(Ze)^2}{R}-\frac{\hbar^2}{2\bar{\nu}}\nabla_r^2-\frac{Ze^2}{\rho}-\frac{Ze^2}{|\boldsymbol{\rho}+\mathbf{R}|}\ , \tag{27}$$

$$\bar{\mu}=\mathcal{M}/2\ , \tag{28a}$$

$$\bar{\nu}=2m\mathcal{M}/(2\mathcal{M}+m)\ , \tag{28b}$$

and $\mathbf{r}$ is shown in Fig. 1, we obtain the usual adiabatic Schrödinger equation for the relative motion in the variable R

$$\left[-\frac{\hbar^2}{\mathcal{M}}\left[\frac{\partial^2}{\partial R^2}+\frac{2}{R}\frac{\partial}{\partial R}\right]+\varepsilon^{JP}(R)+\frac{(Ze)^2}{R}+C_1^{JP}(R)+C_2^{JP}(R)+C_3^{JP}(R)\right]\Phi^{JP}(R)=E\Phi^{JP}(R)\ . \tag{29}$$

The C_1, C_2, and C_3 terms carry the usual adiabatic corrections in addition to the appropriate angular momentum centrifugal barrier in the variable R which is embedded in C_1

$$C_1^{JP}(R)=\left\langle\psi^{JP}\left|\frac{1}{\mathcal{M}}\frac{L^2}{R^2}\right|\psi^{JP}\right\rangle\ , \tag{30}$$

where L^2 is the angular momentum operator in R. Adiabatic corrections in C_1^{JP} are obtained by subtracting

$$\frac{\hbar^2}{\mathcal{M}}\frac{J(J+1)}{R^2}\ ,$$

and depend not only on J but also on the electronic state ψ^{JP} used in (25) (see the Appendix).

Since h and ψ^{JP} involve the separated atom reduced mass [see Eq. (9)] one may write

$$\bar{\nu}^{-1}=m^{-1}+(2\mathcal{M})^{-1}=\nu^{-1}-(2\mathcal{M})^{-1}\ , \tag{31}$$

where

$$\nu^{-1}=m^{-1}+\mathcal{M}^{-1}\ . \tag{32}$$

Therefore C_2 may be written as

$$C_2^{JP}(R)=-\frac{\nu}{2\mathcal{M}}\left\langle\psi^{JP}\left|-\frac{\hbar^2}{2\nu}\nabla_r^2\right|\psi^{JP}\right\rangle\ , \tag{33}$$

which is the usual mass polarization correction to the electronic kinetic energy. The mass polarization correction term C_2 carries here a sign that is different from the convention adopted by Kolos[20] and Beckel *et al.*[21] The difference comes from using the separated atom reduced mass ν in h and ψ^{JP} instead of the electronic mass alone. If one changes ν into m in (50), (9), (12), and (15), one gets a repulsive correction for the mass polarization much like those in Refs. 20 and 21. On the contrary, if one follows our prescription and uses $\nu=m\mathcal{M}(m+\mathcal{M})$ everywhere one gets an attractive correction from C_2. To compare the results of our calculations with those of Refs. 20 and 21 we make $\nu=m$ in (5)–(15).

The third correction term involves the derivatives of ψ with respect to R and may be calculated using some properties of ψ^{JP} and $-i\hbar\partial/\partial R$ which is an Hermitian operator while acting on bound states.[15,16] Since ψ^{JP} is normalized to unity at each R we have

$$C_3^{JP}(R)=\frac{\hbar^2}{\mathcal{M}}\left\langle\frac{\partial}{\partial R}\psi^{JP}\left|\frac{\partial}{\partial R}\psi^{JP}\right\rangle\right.\ , \tag{34}$$

which involves derivatives of ψ with respect to R. In the Appendix we use the work developed in I to write explicit expressions for Eqs. (33) and (34). In the framework of the present Faddeev *Ansatz* for ψ^{JP}, both C_1^{JP} and C_2^{JP} are easy to calculate. Therefore most of the numerical effort goes into obtaining C_3^{JP}, where all derivatives of $\varepsilon^{JP}(R)$ and $G^{JP}(R;c)$ have to be done numerically. Only the derivatives of $\Theta_u^l(\varepsilon;q)$ defined in (A4) with respect to ε may be done analytically since Θ_u^l is a ratio of polynomials in $\delta=\sqrt{-\varepsilon}$. Due to the nature of the electronic *Ansatz* this work is numerically more time consuming than what one usually finds in equivalent quantum-chemistry calculations for H_2^+. Nevertheless, once the effort of programming all necessary steps in the calculation is completed, one has in effect developed an approach that is flexible enough and general enough to deal with different molecular three-body problems in atomic as well as in nuclear physics where the $\mathcal{M}/m$ mass ratio is smaller than $m_p/m_e=2000$, or the potentials are short range and strongly spin dependent.

Coming back to the H_2^+ calculation we show in Table

TABLE VII. $C_2^{0+}(R)$ (in a.u.) vs R for increasing (n_{max},l_{max}). Results from Ref. 20 are given for comparison. For $\bar{\mu}/m_e$ we use 918.06, which is the same as in Kolos's work.

	$10^3C_2^{0+}(R)$ (a.u.)				10^3H_2 (a.u.)
R/a_0	(3,2)	(5,4)	(7,6)	(8,7)	Ref. 20
0.0	0.544 627	0.544 627	0.544 627	0.544 627	0.544 627
0.2	0.493 689	0.493 780	0.493 799	0.493 802	not available
0.4	0.417 750	0.418 067	0.418 103	0.418 107	0.418 113
0.6	0.353 420	0.353 848	0.353 876	0.353 878	0.353 879
0.8	0.303 273	0.303 692	0.303 708	0.303 709	0.303 710
1.0	0.264 536	0.264 880	0.264 891	0.264 892	0.264 892
1.2	0.234 340	0.234 609	0.234 618	0.234 618	0.234 619
1.4	0.210 521	0.210 728	0.210 735	0.210 736	0.210 737
1.6	0.191 518	0.191 681	0.191 688	0.191 689	0.191 689
1.8	0.176 220	0.176 354	0.176 361	0.176 362	0.176 362
2.0	0.163 823	0.163 941	0.163 948	0.163 948	0.163 949
3.0	0.129 197	0.129 313	0.129 317	0.129 318	0.129 317
4.0	0.119 198	0.119 302	0.119 305	0.119 305	0.119 303
5.0	0.120 174	0.120 226	0.120 227	0.120 231	0.120 224
6.0	0.124 914	0.124 905	0.124 905	0.124 905	0.124 902
7.0	0.129 472	0.129 425	0.129 425	0.129 425	0.129 421
8.0	0.132 565	0.132 510	0.132 510	0.132 510	0.132 506
9.0	0.134 331	0.134 285	0.134 285	0.134 285	0.124 281
10.0	0.135 249	0.135 217	0.135 217	0.135 217	0.135 216
15.0	0.136 109	0.136 107	0.136 107	0.136 107	0.136 107
20.0	0.136 145	0.136 145	0.136 145	0.136 145	0.136 145
∞	0.136 157	0.136 157	0.136 157	0.136 157	0.136 157

VII the values we obtain for C_2^{0+} versus R and compare with Kolos's results denoted in Ref. 20 as H_2. The values we obtain for C_2^{0+} converge monotonically to Kolos's results as (n_{max},l_{max}) increases. At (8,7) which corresponds to a 36-term Sturmian basis set, we get six- or seven-digit accuracy at all values of R ranging from $R=0$ to $20a_0$. As in Kolos's calculation $C_2^{0+}(R)$ has a minimum around $R=4.3a_0$. Although we have calculated $C_1^{0+}(R)$ and $C_3^{0+}(R)$ separately we show in Table VIII $C_1^{0+}+C_3^{0+}$ to compare with Kolos's results denoted in Ref. 20 as H_1. Unlike C_2^{0+} or even C_3^{0+}, C_1^{0+} which carries the L^2 matrix elements is very sensitive, not only to the size of the

TABLE VIII. $C_1^{0+}(R)+C_3^{0+}(r)$ vs R for increasing (n_{max},l_{max}). Results from Ref. 20 are given for comparison.

	$10^3[C_1^{0+}(R)+C_3^{0+}(R)]$ (a.u.)					10^3H_1 (a.u.)
R/a_0	(3,2)	(4,3)	(5,4)	(6,5)	(7,6)	Ref. 20
0.4	0.091 05	0.086 70	0.084 02	0.083 04	0.082 40	0.083 27
0.6	0.106 73	0.101 79	0.098 93	0.099 54	0.104 09	0.095 56
0.8	0.112 47	0.107 44	0.104 46	0.109 22	0.114 37	0.098 99
1.0	0.114 36	0.109 50	0.104 39	0.105 32	0.103 30	0.099 05
1.2	0.114 87	0.109 88	0.103 43	0.100 52	0.102 09	0.098 03
1.4	0.114 98	0.109 98	0.102 43	0.101 92	0.104 70	0.096 86
1.6	0.115 08	0.109 97	0.099 89	0.104 32	0.105 18	0.095 92
1.8	0.115 33	0.110 11	0.101 81	0.105 25	0.104 68	0.095 36
2.0	0.115 78	0.110 49	0.105 73	0.101 81	0.100 01	0.095 19
3.0	0.120 80	0.115 88	0.113 62	0.112 57	0.114 88	0.099 84
4.0	0.128 40	0.124 75	0.122 97	0.123 64	0.129 03	0.110 12
5.0	0.135 16	0.132 88	0.131 66	0.131 08	0.137 76	0.120 84
6.0	0.138 82	0.137 54	0.136 82	0.136 40	0.138 68	0.128 38
7.0	0.139 73	0.139 07	0.138 69	0.138 46	0.138 41	0.132 45
8.0	0.139 38	0.139 05	0.138 87	0.138 76	0.138 69	0.134 38
9.0	0.138 72	0.138 57	0.138 49	0.138 44	0.138 58	0.135 29
10.0	0.138 13	0.138 07	0.137 99	0.138 01	0.138 00	0.135 71
15.0	0.136 77	0.136 77	0.136 77	0.136 77	0.136 77	0.136 11
20.0	0.136 42	0.136 42	0.136 42	0.136 42	0.136 42	0.136 15
∞	0.136 16	0.136 16	0.136 16	0.136 16	0.136 16	0.136 16

basis set but also to the accuracy with which the channel weights $G^{0+}(R;ulL)$ are calculated as the number of basis states increases. Therefore for $(n_{\max},l_{\max})>(5,4)$ and $R<8a_0$ the results shown in Table VIII are not reliable. In spite of numerous checks on the algebra and the computer code we are not able to overcome this numerical difficulty.

As we mentioned before, the G's are obtained from the solution of Eq. (11) which is a homogeneous algebraic equation that depends on R and ε. At a given R a solution only exists for a discrete set of ε's, which are those for which the determinant (22) vanishes. Given one of them, say, $\varepsilon_1^{0+}(R)$, which corresponds to $1s\sigma_g$ energies, we look for the eigenvector of $B+v$ corresponding to a zero eigenvalue (the lowest one in actual fact). For that purpose we make use of standard routines from International Mathematical Statistical Library or Numerical Algorithms Group with great success for most choices of $(n_{\max},l_{\max})$ and R. Nevertheless, for $R<8a_0$ and $(n_{\max},l_{\max})>(5,4)$ the resulting G's become unstable when we change the size of the basis set. The numerical difficulties are associated with the $B+v$ matrix having in those cases several eigenvalues very close to zero (ranging from 10^{-2} to 10^{-8}) in addition to one at 10^{-12}. When the lowest eigenvalue is at least a factor of 10^6 smaller than the next one no numerical difficulties are encountered and stable results are obtained for the dominant G's.

Therefore if we limit ourselves to the (5,4) results in Table VIII we find that, much like H_1 in Kolos's calculation, $C_1^0+C_3^{0+}$ goes to zero at $R=0$ and peaks around $R\simeq 0.9a_0$, but fails to have a minimum at $R\simeq 2a_0$ (has one instead at $R\simeq 1.6a_0$) or to increase monotonically as $R\to\infty$ (has instead a second maximum at $R=8a_0$). The minimum at $R\simeq 2a_0$ seems to appear at (6,5) although, as mentioned above, the results are not be trusted.

Provided one is able to overcome the numerical difficulties mentioned above, one could always argue that improved accuracy should result by increasing $(n_{\max},l_{\max})$. Nevertheless, in view of a discrepancy between our results and Kolos's results for $R>8a_0$, we suspect that the choice of adiabatic coordinates $(\rho_K\mathbf{R}_k)$ in (7) instead of correct Jacobi variables $(\rho_K,\mathcal{R}_K)$ shown in Figs. 1(b) and 1(c) may in the end be responsible for a persistent but small discrepancy at all R which naturally shows up in $C_1^{0+}(R)$.

To overcome the problems encountered in the diagonalization of h using (7), we make use of the ideas of Pack and Hirschfelder[13] and diagonalize instead $h+L^2/2\bar{\mu}R^2$ using the same *Ansatz*. This corresponds in part to an improved adiabatic (IA) calculation[15] since the mass polarization matrix elements involving $(-1/4\mathcal{M})\nabla_r^2$ are left out. Including them is not difficult in the present formulation, but since our main concern is the accuracy with which L^2 matrix elements are carried out by the present *Ansatz* we decided not to include them at this time. The new matrix equation for the G's is

$$\sum_c\left[B^{c'c}(R;JP)+v^{c'c}(R;JP)+\frac{\hbar^2}{\mathcal{M}R^2}\sum_{\gamma=0}L_\gamma^{c'c}(R;JP)\right]G^{JP}(R;c)=0\ , \tag{35}$$

where the L_γ are given in (A18), (A20), and (A23) after the G's have been removed. Unlike (11) we find that (35) is extremely well conditioned at all R and choice of $(n_{\max},l_{\max})$ ranging from (2,1) to (8,7). Once the G's are obtained from the solution of (35) new adiabatic corrections $\bar{C}_2^{0+}(R)$ and $\bar{C}_3^{0+}(R)$ may be obtained using (A27) and (A35)–(A40). In Table IX we show the new results for $\bar{C}_2^{0+}(R)$ with $(n_{\max},l_{\max})=(8,7)$ which are less repulsive than the corresponding values shown in Table VII. The difference between the two calculations grows with R and becomes 5×10^{-8} a.u. at $R=20a_0$. Also in Table IX we show $\bar{C}_3^{0+}(R)$ for increasing $(n_{\max},l_{\max})$. Although we have displayed six digits after the decimal point we believe that only the first four or five are accurate due to limitations on the precision with which we calculate the derivatives of the G's. For comparison we also show $C_3^{0+}(R)$ with (8,7). Although $\bar{C}_3^{0+}(R)$ is more repulsive than $C_3^{0+}(R)$ for $R<3a_0$ and less repulsive thereafter, the difference never exceeds 6×10^{-8} a.u. and decreases at large R to become $\simeq 1.1\times10^{-8}$ a.u. at $R=20a_0$. Adding to $\bar{C}_3^{0+}$ the energy difference $\bar{C}_1^{0+}(R)$ between the $1s\sigma_g$ electronic energies obtained from the solution of Eqs. (11) and (35)

$$\bar{C}_1^{0+}(R)=[\varepsilon_1^{0+}(R)]_{(35)}-[\varepsilon_1^{0+}(R)]_{(11)}\ , \tag{36}$$

we get new improved results for the adiabatic corrections associated with L^2 and the derivatives of ψ_1^{0+}. This is shown in Table X for an increasing number of terms in the basis set. As expected from Ref. 15, improved adiabatic results (all orders in the perturbation) are less repulsive than standard ones (first order alone), but in our calculations the greatest change occurs in $\bar{C}_1^{0+}(R)$ relative to $C_1^{0+}(R)$. Because our $C_1^{0+}(R)$ results for $(n_{\max},l_{\max})>(5,4)$ are not reliable, we compare the results of Table X with those of Kolos,[20] which like those of Beckel *et al.*[21] we take to be the benchmark for first-order adiabatic contributions. Although improved adiabatic and standard adiabatic results do not have to coincide, for large heavy-light mass ratio their difference is small and grows with R. In a recent calculation[15] for HD^+ the difference is 1.8×10^{-7} a.u. at $R=5a_0$ and 6.8×10^{-7} a.u. at $r=20a_0$. The difference between our improved adiabatic results with $(n_{\max},l_{\max})=(8,7)$ and Kolos's results grows with R to become 3×10^{-5} a.u. at $R=5a_0$ and decreases thereafter. Our results now develop a minimum at $R\simeq 2a_0$ but show a persistent maximum at $R=10a_0$ and still an exceedingly large difference relative to Kolos's result at $R=20a_0$ (2.4×10^{-7} a.u. more repulsive). Since the present calculation suffers from no ill-conditioned numerical problem,

TABLE IX. $\bar{C}_2^{0+}(R)$ and $\bar{C}_3^{0+}(R)$ vs R for different $(n_{\max},l_{\max})$. $C_3^{0+}(R)$ at (8,7) is given for comparison.

R/a_0	$10^3\bar{C}_2^{0}(R)$ (a.u.) (8,7)	$10^3\bar{C}_3^{0+}(R)$ (a.u.) (4,3)	(6,5)	(8,7)	$10^3C_3^{0+}(R)$ (8,7)
0.0	0.544 627				
0.2	0.493 799	0.044 255	0.044 100	0.044 078	0.044 075
0.4	0.418 100	0.071 384	0.071 211	0.071 185	0.071 185
0.6	0.353 869	0.077 839	0.077 705	0.077 688	0.077 675
0.8	0.303 707	0.076 487	0.076 377	0.076 370	0.076 363
1.0	0.264 880	0.072 717	0.072 625	0.072 623	0.072 613
1.2	0.234 605	0.068 529	0.068 453	0.068 453	0.068 441
1.4	0.210 722	0.064 637	0.064 573	0.064 582	0.064 566
1.6	0.191 675	0.061 265	0.061 208	0.061 235	0.062 211
1.8	0.176 348	0.058 449	0.058 409	0.058 475	0.058 410
2.0	0.163 934	0.056 157	0.056 119	0.056 185	0.056 133
3.0	0.129 296	0.050 616	0.050 614	0.050 678	0.050 645
4.0	0.119 277	0.050 466	0.050 473	0.050 498	0.050 500
5.0	0.120 189	0.051 217	0.051 222	0.051 181	0.051 241
6.0	0.124 859	0.050 745	0.050 751	0.050 695	0.050 758
7.0	0.129 375	0.049 366	0.049 376	0.049 351	0.049 376
8.0	0.132 457	0.048 015	0.048 017	0.048 016	0.048 022
9.0	0.134 231	0.047 065	0.047 062	0.047 064	0.047 078
10.0	0.135 164	0.046 479	0.046 474	0.046 477	0.046 485
15.0	0.136 057	0.045 628	0.045 627	0.045 627	0.045 638
20.0	0.136 095	0.045 480	0.045 480	0.045 480	0.045 491

we have to conclude that such persistent error in the calculation of the L^2 contribution to the potential energy can only be attributed to the choice of adiabatic Jacobi variables in (7) which are not the exact ones for correct angular momentum coupling to total J and P. The wrong choice of Jacobi variables obviously leads to errors that vanish as $R \to 0$ or ∞ but that may be significant at intermediate values of R, as we find here. Although using $(\rho_K, \mathcal{R}_K)$ instead of $(\rho_K, \mathbf{R}_k)$ increases the algebraic work, it will not increase the computational time by a significant amount. In spite of the limitations of the present approach to predicting L^2 energy contributions accurately we calculate next the $2s\sigma_g$-$3d\sigma_g$ cross inhibition gap $\Delta\varepsilon$ for increasing $(n_{\max},l_{\max})$. Using (7) we diagonalize h and $h + L^2/2\bar{\mu}R^2$ in the region around $R = 4a_0$ and calculate the energy gap $\Delta\varepsilon$ in both cases. As report-

TABLE X. Improved adiabatic results $\bar{C}_1^{0+}(R) + \bar{C}_3^{0+}(R)$ vs R for increasing $(n_{\max},l_{\max})$.

R/a_0	$10^3[\bar{C}_1^{0+}(R) + \bar{C}_3^{0+}(R)]$ (a.u.) (3,2)	(5,4)	(7,6)	(8,7)	10^3H_1 (a.u.) Ref. 20
0.2	0.051 984	0.048 457	0.046 961	0.046 576	not available
0.4	0.089 263	0.081 838	0.079 143	0.077 916	0.083 27
0.6	0.104 137	0.094 559	0.088 195	0.085 977	0.095 56
0.8	0.110 769	0.096 560	0.087 953	0.085 968	0.098 99
1.0	0.113 451	0.094 566	0.086 464	0.085 115	0.099 05
1.2	0.114 367	0.091 968	0.085 599	0.082 661	0.098 03
1.4	0.114 681	0.090 945	0.083 535	0.078 997	0.096 86
1.6	0.114 892	0.091 891	0.080 630	0.075 423	0.095 92
1.8	0.115 203	0.093 276	0.077 781	0.072 604	0.095 36
2.0	0.115 687	0.094 025	0.075 492	0.070 918	0.095 19
3.0	0.120 771	0.094 568	0.078 704	0.073 308	0.099 84
4.0	0.128 389	0.106 793	0.086 196	0.077 948	0.110 12
5.0	0.135 144	0.127 665	0.095 131	0.090 253	0.120 84
6.0	0.138 787	0.136 169	0.110 046	0.100 407	0.128 38
7.0	0.139 690	0.138 553	0.118 601	0.107 399	0.132 45
8.0	0.139 331	0.138 817	0.122 976	0.116 451	0.134 38
9.0	0.138 680	0.138 455	0.129 113	0.124 031	0.135 29
10.0	0.138 094	0.138 001	0.135 360	0.137 750	0.135 71
15.0	0.136 740	0.136 739	0.136 739	0.136 716	0.136 11
20.0	0.136 388	0.136 388	0.136 388	0.136 388	0.136 15

TABLE XI. Cross inhibition gap between $2s\sigma_g$ and $3d\sigma_g$ curves obtained from the diagonalization of h and $h+L^2/2\bar{\mu}R^2$ for increasing (n_{max},l_{max}).

		Δε (a.u.)	
N	(n_{max},l_{max})	h	$h+L^2/2\bar{\mu}R^2$
15	(5,4)	1.241×10^{-5}	3.926×10^{-5}
21	(6,5)	3.734×10^{-6}	2.557×10^{-5}
28	(7,6)	1.686×10^{-6}	1.844×10^{-5}
36	(8,7)	2.731×10^{-7}	1.490×10^{-5}
∞	extrapolated graphically		$\simeq1.3\times10^{-5}$

ed earlier, even when we diagonalize h for a given size basis set, we find an energy gap between the two curves, but this gap gets smaller as we increase (n_{max},l_{max}) up to (8,7). On the contrary, when we diagonalize $h+L^2/2\bar{\mu}R^2$ we find that the $2s\sigma_g$-$3d\sigma_g$ cross inhibition gap does not seem to plunge below 10^{-5} a.u. This is shown in Table XI for increasing (n_{max},l_{max}) where N is the total number of basis states. With $N=36$ we get $\Delta\varepsilon_{36}=1.49\times10^{-5}$ a.u. (3.27 cm^{-1}) at $R\simeq4.053\,52a_0$ from the diagonalization of $h+L^2/2\bar{\mu}R^2$. If one graphically extrapolates Δε for $N=\infty$ one gets $\Delta\varepsilon\simeq1.3\times10^{-5}$ a.u. (2.85 cm^{-1}). If instead one diagonalizes h alone Δε seems to go to zero as N increases. This confirms the explanation of Pack and Hirschfelder[13] that L^2 is responsible for breaking the symmetry that leads to curve crossing in the BO approximation.

IV. CONCLUSIONS

Using the Sturmian-Faddeev *Ansatz* that was first developed[7] in studying the two-center Faddeev equations in the adiabatic limit, we have diagonalized the light-particle Hamiltonian h without using any separable representation for the light-heavy potential. In view of the nice factorization properties of the two-center *Ansatz* that the Sturmian separable representation of the light-heavy particle interaction suggests, the diagonalization still involves the solution of an algebraic homogeneous equation whose solution at each R only exists at a discrete set of energies $\varepsilon_i^{JP}(R)$. Although our only approximation consists in using adiabatic Jacobi variables $(\rho_K,\mathbf{R}_K)$ instead of $(\rho_K,\mathcal{R}_K)$ our space-frame two-center wave function carries all conserved quantum numbers of the Hamiltonian H.

When we apply the method to the solution of H_2^+ to obtain first the electronic energies corresponding to $1s\sigma_g$, $2s\sigma_g$, $3d\sigma_g$, $2p\sigma_u$, and $2p\pi_u$ states we get energy results that are accurate to five to nine digits, depending on the values of R and the electronic state chosen. Usually for $R>5a_0$ one gets better than seven-digit accuracy, while in the inner region the accuracy drops to five or six figures alone. For the $1s\sigma_g$ state we calculate, in first-order perturbation theory, all adiabatic corrections resulting from mass polarization, Coriolis coupling due to the angular momentum L^2 in the variable $\mathbf{R}$, and derivatives of the two-center wave function with respect to R. Of all three terms only the L^2 contribution seems to be strongly dependent on the size of the basis set and on the accuracy with which the SF wave function is calculated. The adiabatic contribution due to mass polarization agrees with previous results by Kolos[20] up to five or six significant figures, but the sum of the remaining two adiabatic corrections fails to converge to Kolos's results by as much as 1.2×10^{-5} a.u. Although part of the problem may be attributed to the homogeneous equation becoming ill conditioned when the number of Sturmian basis states increases beyond $N=15$ and $R<8a_0$, the discrepancy at large values of R [2.3×10^{-6} a.u. at $R=10a_0$ with $(n_{max},l_{max})=(5,4)$] suggests that the error may be associated with the use of adiabatic Jacobi variables, instead of the exact ones that are needed to construct an exact eigenstate of the total angular momentum J based on spherical harmonics that depend on the light-heavy relative orbital angular momentum l and light-heavy pair to remaining heavy-particle relative orbital angular momentum L.

To avoid numerical difficulties in the solution of the underlying homogeneous equation, we make use of the ideas expressed in Ref. 13 and diagonalize $h+L^2/2\bar{\mu}R^2$ instead of h alone, leading to an improved adiabatic calculation of the L^2 contribution. The resulting homogeneous equation is extremely well conditioned, leading to the stable results for the G weights as one increases the number of basis states up to $N=36$ for $(n_{max},l_{max})=(8,7)$. The resulting changes in the mass polarization term grow with R and become 5×10^{-8} a.u. at $R=20a_0$. Although our improved adiabatic results and the standard adiabatic results of Kolos need not coincide, the difference we find in the L^2 term is possibly too large. Therefore, for improved accuracy, one needs to use exact Jacobi variables $(\rho_K,\mathcal{R}_K)$ in (7) instead of $(\rho_K,\mathbf{R}_K)$.

Finally, and with a note of caution for the reasons pointed out above, we calculate the L^2 contribution to the $2s\sigma_g$-$3d\sigma_g$ cross inhibition gap by diagonalizing $h+L^2/2\bar{\mu}R^2$ for both states. For $N=36$ we get $\Delta\varepsilon_{36}=1.49\times10^{-5}$ a.u.

Although the present approach to the molecular three-body problem may have its limitations for the solution of H_2^+ that advanced quantum-chemistry methods may excel, it is general enough to deal with any three-body molecularlike system independently of the light-heavy interaction or the heavy-light mass ratio, because it uses a SF two-center wave function that is written up in terms of light-heavy potential Sturmians, carries all conserved quantum numbers of H, and leads to the correct dissociation limits for the molecule. Therefore, if all the accuracy problems we encountered in H_2^+ can be solved, it may even be an attractive method to deal with some atomic molecules such as $dd\mu$ or $pp\pi$. In nuclear physics where uncertainties in the shape and strength of the potential overshadow the need for extremely high accuracy in the numerical solution of the equations, the present *Ansatz* may be successfully used to study a few systems that behave like hadronic molecules. Work in this direction has led to the study of ^{9}Be as a nuclear molecule made up of $\alpha+n+\alpha$.[17]

Another important conclusion from this work relative to I is that the Sturmian-Faddeev two-center *Ansatz* lacks

the accuracy needed to deal with long-range interactions when the weights $G^{JP}(R;c)$ are calculated through the solution of the corresponding adiabatic Faddeev equation where the light-heavy t matrix is represented in a separable form using Sturmians. Nevertheless, if the very same *Ansatz* is used directly to diagonalize the two-center Hamiltonian, a remarkably improved accuracy is obtained without increasing computing time by more than 10%. Progress is underway to test similar ideas in the solution of the full Faddeev equations for the He atoms.

ACKNOWLEDGMENTS

The authors would like to thank R. C. Johnson for useful discussions on how to calculate some of the matrix elements. One of us (A.C.F.) would like to thank J. Peek for supplying additional unpublished information and R. Pack for stimulating criticism of earlier work. He would also like to thank the T5 division at Los Alamos National Laboratory and the Physics Department at the University of Surrey for the hospitality during the course of his stay.

APPENDIX

As mentioned in Sec. III we now make use of the work developed in I to give explicit expressions for C_1^{JP}, C_2^{JP}, and C_3^{JP}. Putting together Eqs. (6), (7), and (9) to write

$$\psi^{JP}(\boldsymbol{\rho},\mathbf{R})=\frac{1}{\sqrt{2}}\sum_c\int\frac{d^3q}{(2\pi)^3}\left[\varepsilon-\frac{\hbar^2}{2\nu}q^2\right]^{-1}n_l\xi_u^l(\varepsilon;q)\times e^{i\mathbf{q}\cdot\boldsymbol{\rho}}[1+\Omega(-1)^L e^{i\mathbf{q}\cdot\mathbf{R}}]\times y_{lL}^{JM_J}(\hat{\mathbf{q}}\,\hat{\mathbf{R}})G^{JP}(R;c)\ , \tag{A1}$$

where $n_l=\sqrt{4\pi}(-i)^l$ and $y_{lL}^{JM_J}(\hat{\mathbf{q}}\,\hat{\mathbf{R}})$ is given by (3) with $Y_{lm}(\hat{\mathbf{q}})$ instead of $Y_{lm}(\hat{\boldsymbol{\rho}})$. Since $\boldsymbol{\rho}=\mathbf{r}-\mathbf{R}/2$ we may write ψ as

$$\psi^{JP}(\mathbf{r},\mathbf{R})=\frac{1}{\sqrt{2}}\sum_c\int\frac{d^3q}{(2\pi)^3}n_l\alpha_c^{JP}(\varepsilon;q)[\mathcal{O}_1+\Omega(-1)^L\mathcal{O}_2]\times y_{lL}^{JM_J}(\hat{\mathbf{q}},\hat{\mathbf{R}})\ , \tag{A2}$$

where

$$\alpha_c^{JP}(\varepsilon;q)=\Theta_u^l(\varepsilon;q)G^{JP}(R;c)\ , \tag{A3}$$

$$\Theta_u^l(\varepsilon;q)=\left[\varepsilon-\frac{\hbar^2}{2\nu}q^2\right]^{-1}\xi_u^l(\varepsilon;q)\ , \tag{A4}$$

and

$$\mathcal{O}_1=e^{i\mathbf{q}\cdot[\mathbf{r}-(1/2)\mathbf{R}]}\ , \tag{A5}$$

$$\mathcal{O}_2=e^{i\mathbf{q}\cdot[\mathbf{r}+(1/2)\mathbf{R}]}\ . \tag{A6}$$

Using (A2) one may first calculate the norm of ψ

$$\langle\psi^{JP}\,|\,\psi^{JP}\rangle=\sum_{c',c}N^{c'c}(R;JP)=1\ , \tag{A7}$$

where the norm matrix N is given by

$$N^{c'c}(R;JP)=\left[N^0(R;c'c)\delta_{l'l}\delta_{L'L}+\Omega\sum_{\mathcal{L}}\chi_{\mathcal{L}}^{JP}(l'L';lL)N_{\mathcal{L}}^0(R;c',c)\right]G^{JP}(R;c')G^{JP}(R;c)\ , \tag{A8}$$

and

$$N^n(R;c'c)=\int\frac{q^2dq}{2\pi^2}q^n\Theta_{u'}^{l'}(\varepsilon;q)\Theta_u^l(\varepsilon;q)\ , \tag{A9}$$

$$N_{\mathcal{L}}^n(R;c'c)=\int\frac{q^2dq}{2\pi^2}q^n\Theta_{u'}^{l'}(\varepsilon;q)\Theta_u^l(\varepsilon;q)j_{\mathcal{L}}(qR)\ . \tag{A10}$$

The angular momentum coefficient χ is given in (16).

Since the L^2 operator acts only on $\hat{\mathbf{R}}$ we write it a

$$L^2=\sum_\mu L_\mu^+L_\mu\ , \tag{A11}$$

such that

$$L_\mu e^{i\mathbf{q}\cdot\mathbf{R}}=\hbar[\mathbf{R}\times\mathbf{q}]_\mu e^{i\mathbf{q}\cdot\mathbf{R}}\ , \tag{A12}$$

$$[\mathbf{R}\times\mathbf{q}]_\mu=\frac{\sqrt{2}}{i}\sum_{\mu_1\mu_2}C^{111}_{\mu_1\mu_2\mu}R_{\mu_1}q_{\mu_2}\ , \tag{A13}$$

and

$$R_{\mu_1}=R\left[\frac{4\pi}{3}\right]^{1/2}Y_{1\mu_1}(\hat{\mathbf{R}})\ , \tag{A14}$$

$$q_{\mu_2}=q\left[\frac{4\pi}{3}\right]^{1/2}Y_{1\mu_2}(\hat{\mathbf{q}})\ . \tag{A15}$$

Likewise,

$$L_\mu Y_{LM}(\hat{\mathbf{R}})=\sqrt{L(L+1)}C^{L\,1\,L}_{M\,\mu\,M+\mu}Y_{LM+\mu}(\hat{\mathbf{R}})\ . \tag{A16}$$

Since L_μ is a linear operator $C_1^{JP}(R)$ becomes the sum of three matrix elements over all channel components

$$C_1^{JP}(R)=\frac{\hbar^2}{\mathcal{M}R^2}\sum_{c',c}\sum_{\gamma=0}^{2}L_\gamma^{c'c}(R;JP)\ . \tag{A17}$$

The first matrix element L_0 is given by

$$L_0^{c'c}(R;JP)=\left[L(L+1)N^0(R;c'c)\delta_{l'l}\delta_{L'L}+\Omega\sum_{\mathcal{L}}\tilde{\chi}_{\mathcal{L}}^{JP}(l'L';lL)N_{\mathcal{L}}^0(R;c'c)\right]G^{JP}(R;c')G^{JP}(R;c)\ , \tag{A18}$$

where

$$\tilde{\chi}_{\mathcal{L}}^{JP}(l'L';lL)=(-1)\sqrt{L'(L'+1)}\sqrt{L(L+1)}\hat{L}'\hat{L}W(LLL'L';1\mathcal{L})\chi_{\mathcal{L}}^{JP}(l'L';lL)\ , \tag{A19}$$

while for L_1 we get

$$L_1^{c'c}(R;JP)=\frac{R}{2}\left[N^1(R;c'c)[\Xi^{JP}(l'L';lL)+\Xi^{JP}(lL;l'L')]+\Omega\sum_{\mathcal{L}}N_{\mathcal{L}}^1(R;c'c)[\Xi_{\mathcal{L}}^{JP}(l'L';lL)+\Xi_{\mathcal{L}}^{JP}(lL;l'L')]\right]G^{JP}(R;c')G^{JP}(R;c)\ , \tag{A20}$$

where

$$\Xi^{JP}(l'L';lL)=x\sqrt{2}\left[\frac{(-1)^{L+L'}-1}{2}\right](-1)^{J+1}\hat{l}'\hat{l}\hat{L}'\hat{L}\hat{1}\begin{bmatrix}l' & 1 & l\\ 0 & 0 & 0\end{bmatrix}\begin{bmatrix}L & 1 & L'\\ 0 & 0 & 0\end{bmatrix}\times\sqrt{L(L+1)}\hat{L}W(11LL;1L')W(l'lL'L;1J)\ , \tag{A21a}$$

$$x=(-1)^{(l+l'+1)/2}\ , \tag{A21b}$$

and

$$\Xi_{\mathcal{L}}^{JP}(l'L';lL)=x\sqrt{2}\hat{\mathcal{L}}^2\hat{l}'\hat{l}\hat{L}'\hat{L}\hat{1}\sum_{K,K'}\hat{K}^2\hat{K}'^2\begin{bmatrix}l' & 1 & K\\ 0 & 0 & 0\end{bmatrix}\begin{bmatrix}K & \mathcal{L} & l\\ 0 & 0 & 0\end{bmatrix}\begin{bmatrix}L' & 1 & K'\\ 0 & 0 & 0\end{bmatrix}\begin{bmatrix}K' & \mathcal{L} & L\\ 0 & 0 & 0\end{bmatrix}\times(-1)^{L'+1}\sqrt{L(L+1)}\hat{L}\sum_{A}\hat{A}^2W(11LL;1A)W(AL'LK';\mathcal{L}1)\begin{Bmatrix}J & l & L\\ l' & K & 1\\ L' & \mathcal{L} & A\end{Bmatrix}\ , \tag{A22a}$$

$$x=(-1)^{(l+l'+\mathcal{L}+1)/2}\ . \tag{A22b}$$

For L_2 we obtain

$$L_2^{c'c}(R;JP)=\frac{R^2}{4}\left[\left[N^2(R;c'c)\delta_{l'l}\delta_{L'L}-\Omega\sum_{\mathcal{L}}\chi_{\mathcal{L}}^{JP}(l'L';lL)N_{\mathcal{L}}^2(R;c'c)\right]-\left[N^2(R;c'c)\Delta^{JP}(l'L';lL)-\Omega\sum_{\mathcal{L}}\Delta_{\mathcal{L}}^{JP}(l'L';lL)N_{\mathcal{L}}^2(R;c'c)\right]\right]G^{JP}(R;c')G^{JP}(R;c)\ , \tag{A23}$$

where

$$\Delta^{JP}(l'L',lL)=(-1)^{(l-l')/2}\left[\frac{1+(-1)^{L+L'}}{2}\right]\hat{l}'\hat{l}\hat{L}'\hat{L}\sum_{K,K'}\hat{K}^2\hat{K}'^2\begin{bmatrix}l' & 1 & K\\ 0 & 0 & 0\end{bmatrix}\begin{bmatrix}l & 1 & K\\ 0 & 0 & 0\end{bmatrix}\times\begin{bmatrix}L & 1 & K'\\ 0 & 0 & 0\end{bmatrix}\begin{bmatrix}L' & 1 & K'\\ 0 & 0 & 0\end{bmatrix}\begin{Bmatrix}J & l' & L'\\ l & K & 1\\ L & 1 & K'\end{Bmatrix}\ , \tag{A24}$$

and

$$\Delta_{\mathcal{L}}^{JP}(l'L';lL)=x\hat{l}'\hat{l}\hat{L}'\hat{L}\hat{\mathcal{L}}^2\sum_{\substack{K,K'\\P,P'}}\hat{K}^2\hat{K}'^2\hat{P}^2\hat{P}'^2\begin{bmatrix}l' & 1 & K\\ 0 & 0 & 0\end{bmatrix}\begin{bmatrix}l & 1 & K'\\ 0 & 0 & 0\end{bmatrix}\begin{bmatrix}L' & 1 & P\\ 0 & 0 & 0\end{bmatrix}\begin{bmatrix}L & 1 & P'\\ 0 & 0 & 0\end{bmatrix}$$
$$\times\begin{bmatrix}P & \mathcal{L} & P'\\ 0 & 0 & 0\end{bmatrix}\begin{bmatrix}K' & \mathcal{L} & K\\ 0 & 0 & 0\end{bmatrix}\sum_A\hat{A}^2W(PP'A1;\mathcal{L}L)W(KK'1A;\mathcal{L}l')$$
$$\times\begin{Bmatrix}K' & A & l'\\ 1 & P & L'\\ l & L & J\end{Bmatrix}(-1)^{A+K'+l}, \tag{A25a}$$

$$x=(-1)^{(l+l'+\mathcal{L})/2}. \tag{A25b}$$

Since at $R=0$ only the $\mathcal{L}=0$ term in L_0 is nonzero one gets $l'=l$, $L'=L$, $\tilde{X}_0^{JP}(lL;lL)=(-1)^L L(L+1)$, and $N^0(c'c)=N_0^0(0;c'c)$. For the $1s\sigma_g$ curve where $l=0$ is the only contributing state at $R=0$, one gets $L=J$ and $P=(-1)^L$. Therefore for $\Omega P=1$ the standard centrifugal barrier $(\hbar^2/\mathcal{M}R^2)J(J+1)$ emerges from (A18) due to the normalization condition (A8). The L_1 term does not contribute at $R=0$ because, being $l=l'$, $L=L'$, and $\mathcal{L}=0$, all 3-j's are zero. Likewise, L_2 gives a zero contribution at the origin due to cancellations of pairs of terms in the first and second large parentheses of (A23). At $R=\infty$ all $N_{\mathcal{L}}^n$ terms vanish and for similar reasons one recovers a pure centrifugal barrier term of the type $(\hbar^2/\mathcal{M}R^2)J(J+1)$ in addition to a constant term $C_1(\infty)$ which can be shown to be

$$C_1(\infty)=\tfrac{1}{4}(1-\tfrac{1}{3})\frac{2\nu}{\mathcal{M}}\left\langle 1s\left|\frac{\hbar^2}{2\nu}q^2\right|1s\right\rangle, \tag{A26}$$

where $|1s\rangle$ is the asymptotic hydrogen wave function and $\frac{1}{3}$ the value of Δ^{JP} given by (A24) with $l'=l=0$ and $L=L'=J$. As shown below, this constant term together with a similar one from $C_3(\infty)$ cancels out the $C_2(\infty)$ contribution. Therefore the method we propose leads to the correct dissociation limit that one needs in very accurate calculations of molecular systems where the heavy particles have a different mass.[16] For molecular energy curves where at $R=0$ or ∞ the dominant l is different from zero one still obtains a centrifugal barrier term, but the way it appears is not as transparent as in the case of $l=0$, because both at $R=0$ and ∞, for $l\neq 0$ and $J\neq 0$, several L's contribute to the L_0 matrix element with different weights.

Next we calculate $C_2^{JP}(R)$ by using (A1) in (33). Since the ∇_r^2 operator only acts on the plane wave in the variable $\mathbf{r}$, one may add and subtract $\varepsilon^{JP}(R)$ to $-(\hbar^2/2\nu)\nabla_r^2$ to obtain

$$C_2^{JP}(R)=-\frac{\nu}{2\mathcal{M}}\left[\epsilon^{JP}(R)+\sum_{c',c}B(R;JP)G^{JP}(R;c')\times G^{JP}(R;c)\right], \tag{A27}$$

where B is given by (12) and (14), It is worth noting that from (33)

$$C_2(\infty)=-\frac{\nu}{2\mathcal{M}}\left\langle 1s\left|\frac{\hbar^2}{2\nu}q^2\right|1s\right\rangle, \tag{A28}$$

is related to the expectation value of the asymptotic kinetic energy for the electronic motion.

Finally we use (34) to obtain $C_3^{JP}(R)$, which involves derivatives of ψ with respect to R. First one writes

$$\frac{\partial}{\partial R}\psi(\mathbf{r},\mathbf{R})=\dot{\psi}_A(\mathbf{r},\mathbf{R})+\dot{\psi}_B(\mathbf{r},\mathbf{R}), \tag{A29}$$

where

$$\dot{\psi}_A=\frac{1}{\sqrt{2}}\sum_c\int\frac{d^3q}{(2\pi)^3}n_1\dot{\alpha}_c(\varepsilon;q)[\mathcal{O}_1+\Omega(-1)^L\mathcal{O}_2]\times y_{lL}^{JM_j}(\hat{\mathbf{q}}\hat{\mathbf{R}}), \tag{A30}$$

$$\dot{\alpha}_c(\varepsilon;q)=\left[\frac{\partial}{\partial\varepsilon}\Theta_u^l(\varepsilon;q)\right]\left[\frac{\partial\varepsilon}{\partial R}\right]G(R;c)+\Theta_u^l(\varepsilon;q)\left[\frac{\partial}{\partial R}G(R;c)\right], \tag{A31}$$

and

$$\dot{\psi}_B=\frac{1}{\sqrt{2}}\sum_c\int\frac{d^3q}{(2\pi)^3}n_l\alpha_c(\varepsilon;q)[\dot{\mathcal{O}}_1+\Omega(-1)^L\dot{\mathcal{O}}_2]\times y_{lL}^{JM_j}(\hat{\mathbf{q}}\hat{\mathbf{R}}). \tag{A32}$$

The derivatives of $\mathcal{O}$ are straightforward to calculate since

$$\dot{\mathcal{O}}=\frac{\partial}{\partial R}e^{i\mathbf{q}\cdot\mathbf{R}}=i(\mathbf{q}\cdot\hat{\mathbf{R}})e^{i\mathbf{q}\cdot\mathbf{R}} \tag{A33}$$

and

$$(\mathbf{q}\cdot\hat{\mathbf{R}})=q\frac{4\pi}{3}\sum_\mu Y_{1\mu}(\hat{\mathbf{q}})Y_{1\mu}^*(\hat{\mathbf{R}}). \tag{A34}$$

Therefore

$$C_3^{JP}(R)=\langle\dot{\psi}_A\,|\,\dot{\psi}_A\rangle+2\langle\dot{\psi}_A\,|\,\dot{\psi}_B\rangle+\langle\dot{\psi}_B\,|\,\dot{\psi}_B\rangle, \tag{A35}$$

where all the norms can be easily calculated using the methods developed above, leading to integrals of the

same type as those obtained for C_1^{JP}. The simplest of all terms in (A35) is the first one,

$$\langle \mathring{\psi}_A \mid \mathring{\psi}_A \rangle = \sum_{c',c} \left[\ddot{N}^{\,0}(R;c'c) + \Omega \sum_{\mathcal{L}} \chi_{\mathcal{L}}^{JP}(l'L';lL) \times \ddot{N}^{\,0}_{\mathcal{L}}(R;c'c) \right] , \tag{A36}$$

where $\ddot{N}^{\,n}$ and $\ddot{N}^{\,n}_{\mathcal{L}}$ are given by (A9) and (A10), respectively, after substituting $\Theta^{l'}_{u'}(\varepsilon;q)$ and $\Theta^{l}_{u}(\varepsilon;q)$ by $\dot{\alpha}_{c'}(\varepsilon;q)$ and $\dot{\alpha}_{c}(\varepsilon;q)$ as given in (A31). With careful programming all these integrals may be done independently of the values of $G^{JP}(R;c)$, $\partial\varepsilon/\partial R$, and $\partial G^{JP}(R;c)/\partial R$, much like in (A8). Nevertheless, to make the notation as simple as possible we wrote it in closed form. Likewise using (A30) and (A32)–(A34) one gets

$$\langle \mathring{\psi}_A \mid \mathring{\psi}_B \rangle = \tfrac{1}{2} \sum_{c',c} \left[\dot{N}^{\,1}(R;c'c) \tilde{\Xi}^{\,JP}(l'L';lL) + \Omega \sum_{\mathcal{L}} \tilde{\Xi}^{\,JP}_{\mathcal{L}}(l'L';lL) \dot{N}^{\,1}_{\mathcal{L}}(R;c'c) \right] , \tag{A37}$$

where $\dot{N}^{\,n}$ and $\dot{N}^{\,n}_{\mathcal{L}}$ are given by (A9) and (A10), respectively, after substituting $\Theta^{l'}_{u'}(\varepsilon;q)$ by $\dot{\alpha}_{c'}(\varepsilon;q)$ and $\Theta^{l}_{u}(\varepsilon;q)$ by $\alpha_c(\varepsilon;q)$,

$$\tilde{\Xi}_{JP}(l'L';lL) = x(-1)^{J+l}\hat{l}'\hat{l}\hat{L}'\hat{L} \begin{bmatrix} l' & 1 & l \\ 0 & 0 & 0 \end{bmatrix} \times \begin{bmatrix} L & 1 & L' \\ 0 & 0 & 0 \end{bmatrix} W(l'lL'L;1J) , \tag{A38a}$$

$$x = (-1)^{(l+l'+1)/2} , \tag{A38b}$$

and

$$\tilde{\Xi}^{\,JP}_{\mathcal{L}}(l'L';lL) = x(-1)^{L+l}\hat{l}'\hat{l}\hat{L}'\hat{L}\hat{\mathcal{L}}^{\,2} \sum_{K,K'} \hat{K}^{\,2}\hat{K}'^{2} \begin{bmatrix} l' & \mathcal{L} & K \\ 0 & 0 & 0 \end{bmatrix} \begin{bmatrix} K & 1 & l \\ 0 & 0 & 0 \end{bmatrix} \begin{bmatrix} L & \mathcal{L} & K' \\ 0 & 0 & 0 \end{bmatrix} \begin{bmatrix} K' & 1 & L' \\ 0 & 0 & 0 \end{bmatrix} \begin{Bmatrix} J & l' & L' \\ l & K & 1 \\ L & \mathcal{L} & K' \end{Bmatrix} , \tag{A39a}$$

$$x = (-1)^{(l+l'+\mathcal{L}+1)/2} . \tag{A39b}$$

Finally, for the last term in (A35) we obtain

$$\langle \mathring{\psi}_B \mid \mathring{\psi}_B \rangle = \tfrac{1}{4} \sum_{c',c} \left[N^2(R;c'c)\Delta^{JP}(l'L';lL) - \Omega \sum_{\mathcal{L}} \Delta^{JP}_{\mathcal{L}}(l'L';lL) N^2_{\mathcal{L}}(R;c'c) \right] G^{JP}(R;c') G^{JP}(R;c) , \tag{A40}$$

where N^n and $N^n_{\mathcal{L}}$ are given by (A9) and (A10) and the Δ's by (A24) and (A25). Since all $N_{\mathcal{L}}$'s vanish at $R \to \infty$, and $\partial\varepsilon/\partial R$ and $\partial G/\partial R$ go to zero as $R \to \infty$, at $R = \infty$ only a constant term in $\langle \mathring{\psi}_B \mid \mathring{\psi}_B \rangle$ remains. For the $1s\sigma_g$ curve, for reasons similar to those pointed out above for $C_1(R)$, we get

$$C_3(\infty) = \frac{1}{4}\frac{1}{3}\frac{2\nu}{\mathcal{M}} \left\langle 1s \left| \frac{\hbar^2}{2\nu} q^2 \right| 1s \right\rangle . \tag{A41}$$

Therefore $C_1(\infty) + C_2(\infty) + C_3(\infty) = 0$, assuming one uses ν instead of m in the appropriate places.

*Permanent address: Centro de Física Nuclear, Avenida do Professor Gama Pinto 2, 16699 Lisboa, Codex, Portugal.

[1] A. C. Fonseca and P. E. Shanley, Ann. Phys. (N.Y.) **117**, 268 (1979).
[2] A. C. Fonseca and P. E. Shanley, Nucl. Phys. A **382**, 97 (1982).
[3] A. C. Fonseca, in *Resonances-Models and Phenomena*, Vol. 211 of *Lecture Notes in Physics*, edited by S. Albererio, L. S. Ferreira, and S. Streit (Springer-Verlag, Berlin, 1984), p. 192.
[4] A. C. Fonseca, J. Revai, and A. Matveenko, Nucl. Phys. A **326**, 182 (1979); J. Revai and A. Matveenko, *ibid.* **339**, 448 (1980).
[5] A. C. Fonseca, E. F. Redish, and P. E. Shanley, Nucl. Phys. A **320**, 273 (1979).
[6] R. A. Buckingham, in *Quantum Theory*, edited by D. R. Bates (Academic, New York, 1961), Vol. 1, Chap. 3.
[7] A. C. Fonseca and M. T. Peña, Phys. Rev. A **36**, 4585 (1987).
[8] S. Weinberg, Phys. Rev. **131**, 440 (1963).
[9] D. R. Bates, K. Ledsham, and A. L. Steward, Philos. Trans. R. Soc. London, Ser. A **246**, 215 (1953); H. Wind, J. Chem. Phys. **42**, 2371 (1965).
[10] M. M. Madsen and J. M. Peek, At. Data **2**, 171 (1971).
[11] D. M. Bishop and L. M. Cheung, Phys. Rev. A **16**, 640 (1977), and references therein.
[12] A. C. Fonseca and M. T. Peña, in *Few-Body Systems, Supplementum 2*, edited by J. L. Ballot and M. Fabre de la Ripelle (Springer-Verlag, Vienna, 1987).
[13] R. T. Pack and J. O. Hirschfelder, J. Chem. Phys. **49**, 4009 (1968); **52**, 521 (1970); **52**, 4198 (1970).
[14] S. Weinberg, Phys. Rev. **133**, B232 (1964).
[15] R. T. Pack, Phys. Rev. A **32**, 2022 (1985).
[16] M. C. Struensee, J. S. Cohen, and R. T. Pack, Phys. Rev. A **34**, 3605 (1986).
[17] A. C. Fonseca and M. T. Peña, Nucl. Phys. A (to be published).
[18] W. K. Ford and F. S. Levin, Phys. Rev. A **29**, 30 (1984); **29**, 43

(1984).
[19]W. Plessas, in *Models and Methods in Few-Body Physics,* Vol. 273 of *Lecture Notes in Physics,* edited by L. S. Ferreira, A. C. Fonseca, and L. Streit (Springer-Verlag, Heidelberg, 1987), p. 137.
[20]W. Kolos, Acta Phys. Acad. Sci. Hung. **27**, 241 (1969).
[21]C. L. Beckel, B. D. Hausen, and J. M. Peek, J. Chem. Phys. **53**, 3681 (1970).